Brain Networks and Cognitive Impairment in Parkinson's Disease

Rosaria Rucco,[1,2,*,i] Anna Lardone,[3,*] Marianna Liparoti,[1] Emahnuel Troisi Lopez,[1,ii]
Rosa De Micco,[4] Alessandro Tessitore,[4] Carmine Granata,[2] Laura Mandolesi,[5]
Giuseppe Sorrentino,[1,2,6] and Pierpaolo Sorrentino[2,7]

Abstract

Aim: The aim of the present study is to investigate the relationship between both functional connectivity and brain networks with cognitive decline, in patients with Parkinson's disease (PD).

Introduction: PD phenotype is not limited to motor impairment but, rather, a wide range of non-motor disturbances can occur, with cognitive impairment being one of the most common. However, how the large-scale organization of brain activity differs in cognitively impaired patients, as opposed to cognitively preserved ones, remains poorly understood.

Methods: Starting from source-reconstructed resting-state magnetoencephalography data, we applied the phase linearity measurement (PLM) to estimate functional connectivity, globally and between brain areas, in PD patients with and without cognitive impairment (respectively PD-CI and PD-NC), as compared with healthy subjects (HS). Further, using graph analysis, we characterized the alterations in brain network topology and related these, as well as the functional connectivity, to cognitive performance.

Results: We found reduced global and nodal PLM in several temporal (fusiform gyrus, Heschl's gyrus, and inferior temporal gyrus), parietal (postcentral gyrus), and occipital (lingual gyrus) areas within the left hemisphere, in the gamma band, in PD-CI patients, as compared with PD-NC and HS. With regard to the global topological features, PD-CI patients, as compared with HS and PD-NC patients, showed differences in multi-frequencies bands (delta, alpha, gamma) in the Leaf fraction, Tree hierarchy (Th) (both higher in PD-CI), and Diameter (lower in PD-CI). Finally, we found statistically significant correlations between the Montreal Cognitive Assessment test and both the Diameter in delta band and the Th in the alpha band.

Conclusion: Our work points to specific large-scale rearrangements that occur selectively in cognitively compromised PD patients and are correlated to cognitive impairment.

Keywords: brain networks topology; cognition; functional connectivity; graph theory; magnetoencephalography; synchrony

Impact Statement

In this article, we want to test the hypothesis that the cognitive decline observed in Parkinson's disease (PD) patients may be related to specific changes of both functional connectivity and brain network topology. Specifically, starting from magnetoencephalography signals and by applying the phase linearity measurement (PLM), a connectivity metric that measures the synchronization between brain regions, we were able to highlight differences in the global and nodal PLM values in PD

[1]Department of Motor Sciences and Wellness, University of Naples Parthenope, Naples, Italy.
[2]Institute for Applied Science and Intelligent Systems, National Research Council, Pozzuoli, Italy.
[3]Department of Social and Developmental Psychology, University of Rome "Sapienza," Rome, Italy.
[4]Department of Advanced Medical and Surgical Sciences, University of Campania "Luigi Vanvitelli," Naples, Italy.
[5]Department of Humanistic Studies, University of Naples Federico II, Naples, Italy.
[6]Hermitage-Capodimonte Hospital, Naples, Italy.
[7]Institut de Neurosciences des Systèmes, Aix-Marseille University, Marseille, France.
*These authors contributed equally to the article.
[i]ORCID ID (https://orcid.org/0000-0003-0943-131X).
[ii]ORCID ID (https://orcid.org/0000-0002-0220-2672).

patients with cognitive impairment as compared with both cognitively unimpaired patients and healthy subjects. Further, using graph analysis, we analyzed alterations in brain network topology that were related to cognitive functioning.

Introduction

U NLIKE WHAT JAMES Parkinson claimed more than 200 years ago about the disease bearing his name (''the senses and intellects being uninjured'') (Walshe, 1961), today we know that Parkinson's disease (PD) is not solely a motor disease (Vitale et al., 2012). Indeed, PD is characterized by a broad spectrum of non-motor symptoms, including neuropsychiatric disturbances, autonomic dysfunctions, and cognitive decline. After 20 years of disease duration, up to 80% of patients present with severe cognitive symptomatology (Aarsland et al., 2009). However, despite extensive investigation, the pathophysiological mechanisms underlying cognitive decline remain unclear (Aarsland and Kurz, 2010).

In the early stage of the disease, the brainstem and the surviving neurons of the nigrostriatal dopamine system are mostly affected by alpha synuclein depositions whereas, with disease progression, the neuropathological process spreads to other brain regions, including the cortex (Braak et al., 2003). Hence, PD may be regarded as a whole-brain disease.

Cognitive functions need coordinated interactions between multiple brain areas. Synchronization is one of the putative mechanisms of information routing across brain areas (Buzsáki and Draguhn, 2004). Accordingly, different electroencephalographic or magnetoencephalographic (MEG) studies observed a relationship between neural synchrony and cognitive functions (Singer, 1999; Varela et al., 2001).

Graph theory is a mathematically principled way to represent complex interactions among multiple elements. In this context, brain areas are represented as nodes, and their interactions are the links (Rubinov and Sporns, 2010; Sporns et al., 2005). Measuring topological features of the brain networks is informative about the large-scale organization underpinning cognitive processes. Recently, the graph theory has been applied to MEG signals in neurodegenerative diseases, demonstrating alterations in structural organization (Pievani et al., 2014) as well as in brain functional networks, such as in amyotrophic lateral sclerosis (Sorrentino et al., 2018), hereditary spastic paraplegia (Rucco et al., 2019), and mild cognitive impairment (Jacini et al., 2018).

Given its high spatiotemporal resolution, MEG is a useful tool for detecting the evolution of brain functional connectivity. The MEG systems measure the magnetic fields produced by neuronal activity, which are undistorted by the layers surrounding the brain. Therefore, it is possible to reconstruct the neural signals produced by different brain areas (source space) (Baillet, 2017). In particular, MEG has a millisecond temporal resolution, making it possible to study frequency-specific networks, and records the oscillatory activity of brain regions, allowing to estimate the phase of brain signals and, hence, synchronization (Varela et al., 2001). Typically, the canonical frequency bands (delta, theta, alpha, beta, and gamma) are taken into account to understand the cognitive processes (Lopes da Silva, 2013).

Stoffers and associates (2007) have analyzed the MEG signals during resting state in a group of *de novo* PD pa-

tients, finding changes in brain activity, which included a widespread increase in theta and low alpha power, and a loss of beta and gamma power. However, they did not find correlations between brain activity and disease duration, disease stage (i.e., Hoehn and Yahr [H&Y]) (Hoehn and Yahr, 1967) and disease severity (i.e., Unified Parkinson's Disease Rating Scale [UPDRS-III]) (Fahn, 1987). The authors hypothesized that the spectral power changes may be linked to the degeneration of non-dopaminergic ascending neurotransmitter systems. It has been demonstrated, especially in functional magnetic resonance imaging (MRI) studies, that the disruption of resting-state functional connectivity is important in the development of cognitive decline in PD (Amboni et al., 2018; Tessitore et al., 2012a).

Some studies have compared, using MEG, the brain activity of non-demented and demented PD patients with that of matched healthy subjects (HS). All in all, a general trend was found toward the slowing of resting brain activity in demented and (to a lesser extent) non-demented patients, as compared with HS. This slowing of oscillatory brain activity can be interpreted as a mechanism related to the progression of the disease and may be potentially involved in the development of dementia in PD (Bosboom et al., 2006; Dubbelink et al., 2013).

In a source-level, resting-state MEG study, Olde Dubbelink and associates (2014) found pathologically altered functional networks in *de novo* PD patients, which can be interpreted as a reduction in local integration with preserved overall efficiency of the brain network. Further, they have analyzed longitudinally 43 PD patients also, discovering progressive impairment in local integration in multiple frequency bands and loss of global efficiency in the PD brain network, related to a worse performance in the Cambridge Cognition Examination (CAMCOG) scale (a test assessing the global cognitive function) (Roth et al., 1986).

Ultimately, starting from the observation that the synchronization in specific frequency bands between different brain areas is the basis of a variety of cognitive processes, our hypothesis is that in PD there could be abnormal neuronal synchronization that is reflected in changes in functional connectivity and, possibly, in the topological features of the brain networks. More specifically, we hypothesize that, in PD, the progressive alteration of the brain networks would be more pronounced in patients with clinically evident cognitive impairment, as compared with cognitively unimpaired patients.

To test our hypotheses, we performed a resting-state MEG recording in PD patients with and without cognitive impairment, and age- and sex-matched HS. We estimated synchronization between the brain source-reconstructed time series by using the phase linearity measurement (PLM) (Baselice et al., 2019). We then applied the minimum spanning tree (MST) algorithm (Tewarie et al., 2015) to reconstruct the brain networks, and we analyzed functional connectivity among both brain areas and topological features of the network. Finally, we correlated our results to clinical motor, cognitive, and behavioral PD-specific scales.

Materials and Methods

Participants

Thirty-nine early PD patients were diagnosed according to the modified diagnostic criteria of the UK Parkinson's Disease Society Brain Bank (Gibb and Lees, 1988) and recruited at the Movement Disorders Unit of the First Division of Neurology at the University of Campania "Luigi Vanvitelli" (Naples, Italy). All subjects were right-handed and native Italian speakers.

Inclusion criteria were: (1) PD onset after the age of 40 years, to exclude early onset parkinsonism; (2) a modified H&Y stage ≤2.5. Exclusion criteria were: (1) dementia associated with PD according to consensus criteria (Emre et al., 2007); (2) any other neurological disorder or clinically significant or unstable medical condition; and (3) any contraindications to MRI or MEG recordings. Disease severity was assessed by using the H&Y stages and the UPDRS III. Motor clinical assessment was performed in the "off-state" (off-medication overnight). Levodopa equivalent daily dose (LEDD) was calculated for both dopamine agonists and dopamine agonists + L-dopa (total LEDD) (Tomlinson et al., 2010).

Global cognition was assessed by means of Montreal Cognitive Assessment (MoCA) (Nasreddine et al., 2005). The MoCA consists of 12 subtasks exploring the following cognitive domains: (1) memory (score range 0–5), assessed by means of delayed recall of five nouns, after two verbal presentations; (2) visuospatial abilities (score range 0–4), assessed by a clock-drawing task (3 points) and by copying of a cube (1 point); and (3) executive functions (score range 0–4), assessed by means of a brief version of the Trail Making B task (1 point).

The patients were classified in two groups based on their age- and education-adjusted Italian cut-off MoCA score (Conti et al., 2015). According to these criteria, we selected 20 and 19 PD patients with MoCA score, respectively lower/equal (PD with cognitive impairment, PD-CI) or higher (PD with normal cognition, PD-NC) than the cut-off of 23. Depressive and apathy symptoms were assessed with the Beck Depression Index (BDI) (Beck et al., 1961) and the Apathy Evaluation Scale (AES) (Marin et al., 1991), respectively.

Twenty HS, matched for age, education, and sex, were also enrolled (Table 1).

The study was approved by the local Institutional Human Research Ethics Committee, and it was conducted in accordance to the Declaration of Helsinki. All participants signed informed consent.

MRI acquisition

The MR images were acquired on a 3-T scanner equipped with an 8-channel parallel head coil (General Electric Healthcare, Milwaukee, WI, USA) either after, or a minimum of 21 days (but not more than 1 month) before the MEG recording. Three-dimensional T1-weighted images (gradient-echo sequence Inversion Recovery prepared Fast Spoiled Gradient Recalled-echo, time repetition = 6988 msec, TI = 1100 msec, TE = 3.9 msec, flip angle = 10, voxel size = 1 ×1 ×1.2 mm^3) were acquired.

MEG acquisition

The MEG system acquires the signals of 163 magnetometers placed in a magnetically shielded room (AtB Biomag, Ulm, Germany). Specifically, 154 sensors cover the entire head of the subject; the remaining ones, organized into three orthogonal triplets, are positioned more distant from the helmet and used to measure and reduce the environmental noise (Lardone et al., 2018; Sorrentino et al., 2017). The MEG data were acquired during two, eyes-closed, resting-state segments, each 3.5 min long. The patients were in the off-state (i.e., after drug withdrawal for 24 h, without the effects of the therapy).

TABLE 1. DEMOGRAPHIC AND CLINICAL FEATURES OF PARKINSON'S DISEASE PATIENTS AND HEALTHY SUBJECTS

	PD-CI (n = 20), mean ± SD	PD-NC (n = 19), mean ± SD	HS (n = 20), mean ± SD	p
Age	67.90 ± 8.73	61.00 ± 7.73	63.10 ± 8.53	p = 0.04
Sex (M/F)	10/10	6/13	11/9	NS*
Disease duration (months)	31.00 ± 13.66	35.16 ± 16.36	—	NS
H&Y stage	1.88 ± 0.50	1.82 ± 0.44	—	NS
UPDRS III	26.40 ± 11.03	23.58 ± 7.08	—	NS
MoCA (total)	19.96 ± 2.30	25.05 ± 1.63	—	<0.001
Memory	0.70 ± 0.90	2.32 ± 1.49	—	<0.001
Visuospatial abilities	1.75 ± 0.99	3.16 ± 0.93	—	<0.001
Executive functions	1.35 ± 1.28	3.37 ± 0.58	—	<0.001
Attention, concentration, and working memory	4.35 ± 1.49	5.58 ± 0.67	—	<0.001
Language	4.30 ± 1.23	5.58 ± 0.67	—	<0.001
Spatiotemporal orientation	5.85 ± 0.36	5.89 ± 0.45	—	NS
BDI	5.00 ± 5.23	5.37 ± 6.87	—	NS
Apathy	30.25 ± 7.14	29.79 ± 6.32	—	NS
LEDD total	309.50 ± 159.95	269.21 ± 136.56	—	NS
LEDD DA	67.00 ± 145.64	90.26 ± 103.50	—	NS

Data are expressed as mean ± SD. Age was statistically significant different only between PD-CI and PD-NC, with a p = 0.04.

BDI, Beck Depression Index; DA, dopamine-agonist; HS, healthy subjects; H&Y, Hoehn & Yahr; LEDD, Levodopa equivalent daily dose; MoCA, Montreal Cognitive Assessment; NS*, not significant among the three groups; NS, not significant between PD-CI and PD-NC; PD-CI, Parkinson's disease patients with cognitive impairment; PD-NC, Parkinson's disease patients without cognitive impairment; SD, standard deviation; UPDRS, Unified Parkinson's Disease Rating Scale.

To reconstruct the position of the head in the helmet during the MEG, we digitalized, before acquisition, the position of four reference coils (attached to the head of the subject) and four anatomical landmarks (nasion, right, and left preauricular and apex) using Fastrak (Polhemus®). The coils were activated before each segment of the registration. During the MEG acquisition, electrocardiographic (ECG) and electrooculographic (EOG) signals were also recorded to remove physiological artefact (Gross et al., 2013; Rucco et al., 2019). After an anti-aliasing filter, the data were sampled at 1024 Hz.

Preprocessing

The MEG data were filtered in the band 0.5–48 Hz by using a fourth-order Butterworth IIR band-pass filter, implemented offline by using Matlab scripts within the Fieldtrip toolbox (Oostenveld et al., 2011). To reduce the environmental noise, Principal Component Analysis was used (de Cheveigné and Simon, 2007; Sadasivan, 1996).

Subsequently, an experienced rater identified the noisy channel/segments of acquisition through visual inspection. On average, 140 ± 4 channels were used. The selected channels were shown to be able to reconstruct the anatomical sources, by means of the beamforming algorithm employed (see Source reconstruction section), without any appreciable loss of the reconstruction quality. After that, Independent Component Analysis (Barbati et al., 2004) was performed to identify and remove ECG (typically 1–2 two components) and EOG (0–1 components) signals from the MEG data.

Source reconstruction

The subject's anatomical landmarks were visually identified on the native MRI of the subjects and used to co-register the MEG acquisition, which was then spatially normalized to a template MRI.

Subsequently, the time series related to the centroids of 116 regions-of-interest (ROIs), derived by the Automated Anatomical Labeling (AAL) atlas (Gong et al., 2009; Tzourio-Mazoyer et al., 2002) were reconstructed based on Nolte's volume conduction model (Nolte, 2003) and the Linearly Constrained Minimum Variance (LCMV) beamformer algorithm (Van Veen et al., 1997). However, we considered only the first 90 ROIs, excluding those representing the cerebellum, given the low reliability of the reconstructed signal in those areas. For each ROI, we projected the time series along the dipole direction, which explained most variance by means of singular value decomposition, using Fieldtrip toolbox (Oostenveld et al., 2011).

The beamformer estimates the temporal series representing the activity of the brain regions. Such signals are filtered in the five canonical frequency bands (delta [0.5–4 Hz], theta [4.0–8.0 Hz], alpha [8.0–13.0 Hz], beta [13.0–30.0 Hz], and gamma [30.0–48.0 Hz]), and they are analyzed separately.

Connectivity analysis

To evaluate the synchronization between brain regions, we adopted the PLM (Baselice et al., 2019). This novel, undirected metric, developed by our group, measures the synchronization between brain regions, exploiting the power spectrum of their phase differences in time. It is defined as follows:

$$PLM = \frac{\int_{-B}^{B} \left| \int_0^T e^{i\Delta\emptyset(t)} e^{-i2\pi f\, t} dt \right| 2\, df}{\int_{-\infty}^{\infty} \left| \int_0^T e^{i\Delta\emptyset(t)} e^{-i2\pi f\, t} dt \right| 2\, df}, \qquad (1)$$

where the $\Delta\emptyset(t)$ represents the phase difference between two signals, $2B$ is the integration band, f is the frequency, and T is the observation time interval. The PLM ranges between 0 and 1, where 1 indicates perfect synchronization and 0 indicates non-synchronous activity.

Based on PLM, we obtained a 90×90 weighted adjacency matrix for each temporal series (with a duration >4 sec), for each subject, in each frequency band.

Starting from these weighted adjacency matrices, we calculated, for each ROI, the nodal PLM for each ROI as the average PLM between a specific ROI and all other ROIs, and the global PLM as the average of all nodal PLM values. It is important to note that the PLM value represents the mean connectivity measure of a node, and it is not a graph theoretical metric.

Network analysis

Starting from the weighted adjacency matrices, we reconstructed, based on the MST algorithm, a binary network, where the 90 areas of the AAL atlas are the nodes and the entries represent the edges.

Although several approaches have been proposed in the literature (Fallani et al., 2017), we have chosen the MST algorithm because it allows for an unbiased comparison of the topology of the networks (Tewarie et al., 2015), building a single subgraph that connects all the nodes without forming loops. It allows to calculate statistically comparable metrics, while maintaining most of the information of the original network (Tewarie et al., 2015).

To describe the network, we computed nodal centrality measures (degree, betweenness centrality [BC]) and global, non-centrality (leaf fraction [Lf], degree divergence, diameter, tree hierarchy [Th]) metrics (Stam et al., 2014; Tewarie et al., 2015). The degree of a node is defined as the number of links incident on a given node. The BC is the number of shortest paths passing through a given node over all the shortest paths of the network (Freeman, 1977). The Lf is the fraction of leaf nodes in the MST, where a leaf node is defined as a node with degree one (Boersma et al., 2013). The degree divergence (K) measures the broadness of the degree distribution (Tewarie et al., 2015). The diameter is defined as the longest shortest path of the MST. Lastly, the Th is the number of leaves over the maximum BC.

Statistical analysis

To test differences in age and sex among the three groups, we use analysis of variance (ANOVA) and the Chi-square, respectively, after checking the normal distribution of variables. Clinical parameters, between PD-CI and PD-NC patients, were compared by using t-test.

The three groups were compared for each variable of interest (connectivity and topological metrics) by using the permutational analysis of variance (PERMANOVA), a nonparametric test to evaluate the effect of cognitive impairment on brain connectivity, in PD-CI, PD-NC patients and in controls. Then, all the p-values were corrected by using the

false discovery rate (FDR) (Benjamini and Hochberg, 1995), so as to account for multiple comparisons between the variables. For the significant p-values (after FDR correction), *post hoc* analysis was carried out, using Scheffe's correction for multiple comparisons among groups.

To correlate the connectivity and topological metrics with the clinical scales, we used the Spearman's rank correlation coefficient. Further, to investigate the possible presence of a connectome or a topological networks-based model to predict the cognitive state of the patients (Amico and Goñi, 2018; Shen et al., 2017), we performed a multivariate regression analysis.

All statistical analyses were performed by using custom scripts written in Matlab version 2018a. The significance level was set at $p < 0.05$.

Results

Population characteristics

The studied population consists of 20 PD-CI, 19 PD-NC patients and 20 HS. The gender among the three groups showed no significant difference. The PD-NC patients were slightly younger than PD-CI patients ($p = 0.04$), whereas no differences were found in terms of disease duration, disease stage (i.e., H&Y stage), motor impairment (i.e., UPDRS III), depression (i.e., BDI scale), and apathy (i.e., AES) between the two PD subgroups. As expected, significant differences were found in terms of MoCA scale and its subtests between PD-CI and PD-NC patients (Table 1).

MEG data

Connectivity analysis. Regarding the global PLM value, we found a statistically significant difference in the gamma band among the groups with a $p = 0.0416$ [H (2,58) = 3.365], with *post hoc* analysis showing that PD-CI patients differed from HS, having lower global PLM (Fig. 1).

When we compared the nodal PLM values among the three groups, we found differences in the gamma band in the following areas of the left hemisphere: postcentral gyrus [H (2,58) = 6.578, $p = 0.002$, pFDR = 0.039], lingual gyrus [H (2,58) = 7.563, $p = 0.001$, pFDR = 0.039], fusiform gyrus [H (2,58) = 9.279, $p < 0.001$, pFDR = 0.036], Heschl's gyrus [H (2,58) = 6.985, $p = 0.002$, pFDR = 0.039], and inferior temporal gyrus [H (2,58) = 7.377, $p = 0.001$, pFDR = 0.039]. In the *post hoc* analysis, PD-CI patients showed a lower PLM value with respect to HS in all significant ROI, whereas PD-NC patients only reached statistical significance in the left lingual and the left fusiform areas, as shown in Figure 2.

Topological network analysis. We found topological differences in the brain networks among PD-CI, PD-NC, and HS, in different frequency bands. With respect to Lf, differences appeared in the delta [H (2,58) = 4.732, $p = 0.012$, pFDR = 0.049], the alpha [H (2,58) = 4.371, $p = 0.017$, pFDR = 0.028], and the gamma band [H (2,58) = 7.052, $p = 0.002$, pFDR = 0.012]. *Post hoc* analysis showed that, in all the three bands, PD-CI patients had higher Lf as compared with HS, as depicted in Figure 3.

The Th differed among the three groups in the alpha [H (2,58) = 5.329, $p = 0.006$, pFDR = 0.016] and the gamma
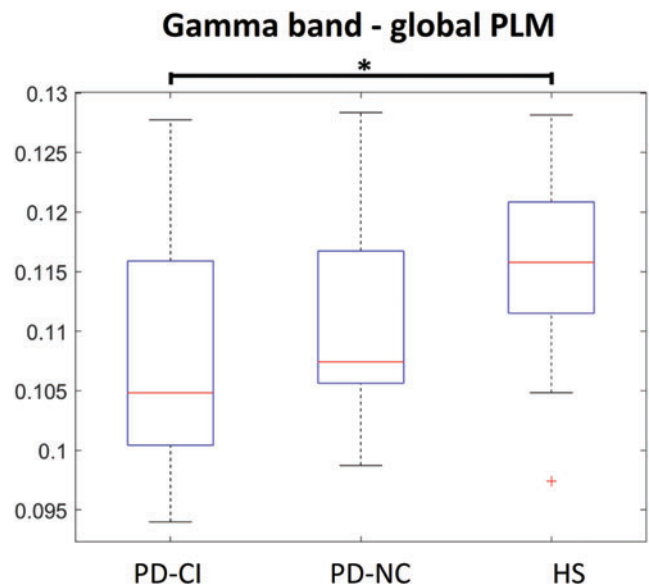

FIG. 1. Differences in the global PLM value among PD-CI, PD-NC, and HS. The box plots refer to differences in the global PLM value in gamma band among PD-CI, PD-NC and HS. The upper and lower bound of the box refer to the 25th to 75th percentiles, the median value is represented by the horizontal line inside each box, the whiskers extend to the 10th and 90th percentiles, and further data are considered as outliers and represented by the symbol +. The PD-CI group shows a lower global PLM value as compared with both PD-NC group (without reaching statistical significance) and HS (*$p < 0.05$). HS, healthy subjects; PLM, phase linearity measurement; PD-CI, Parkinson's disease patients with cognitive impairment; PD-NC, Parkinson's disease patients without cognitive impairment. Color images are available online.

band [H (2,58) = 5.523, $p = 0.007$, pFDR = 0.019]. In the *post hoc* analysis, both PD-CI and PD-NC patients differed from HS with a higher Th in the alpha band, but only PD-CI patients differed from the HS in the gamma band, as reported in Figure 4.

The diameter was statistically different in the delta band [H (2,58) = 4.214, $p = 0.019$, pFDR = 0.049] among the three groups, and in particular between PD-CI patients and HS (Fig. 5).

However, it is to be noted that, although most of the parameters in the PD-NC group did not reach statistical significance, a trend seems evident nonetheless, such that cognitively unimpaired patients show intermediate values between healthy controls and cognitively compromised patients. No statistically significant difference was found among the three groups in the K, the other global topological parameters calculated, and in the centrality parameters, in beta and theta bands (Azarpaikan et al., 2014).

Correlations and multivariate regression analysis. As shown in Figure 6, we found a statistically significant correlation between the MoCA total score and both the diameter in delta band ($R = 0.352$, $p = 0.028$) and the Th in the alpha band ($R = -0.374$, $p = 0.019$). No other statistically significant correlation between connectivity metrics and clinical scales was found.
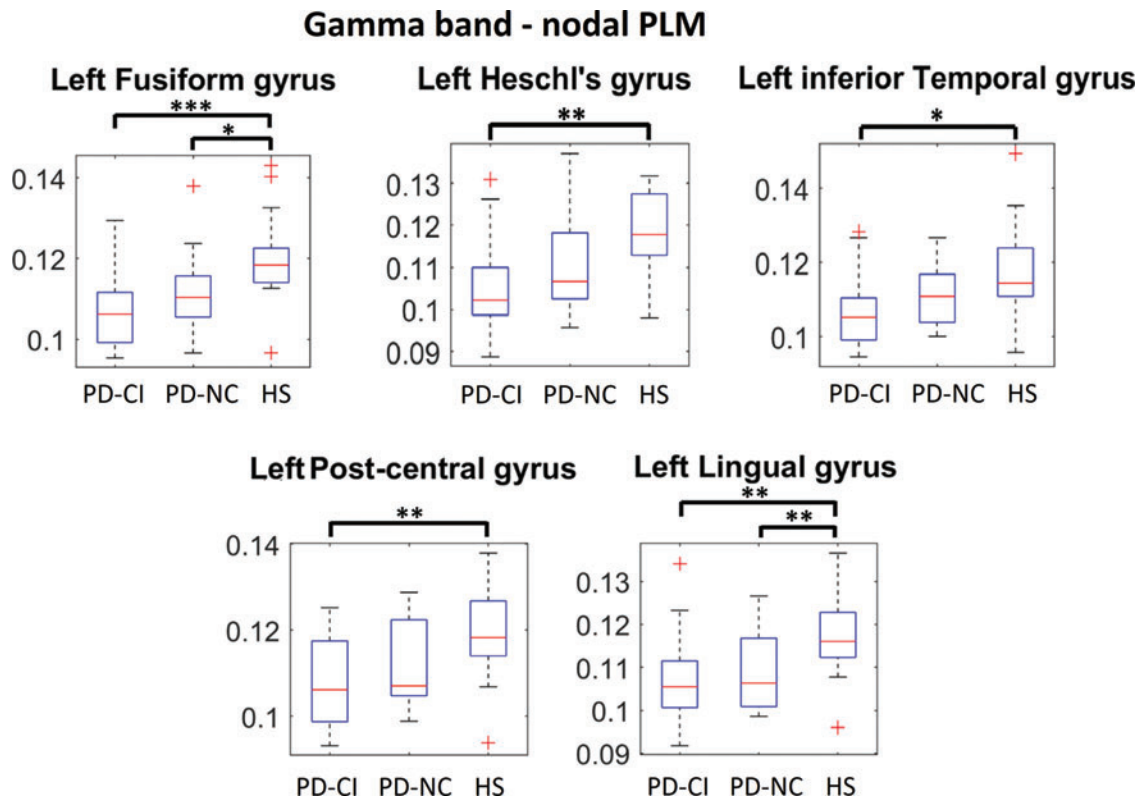
Gamma band - nodal PLM

FIG. 2. Differences in the nodal PLM values among PD-CI, PD-NC, and HS. The box plots refer to differences in the nodal PLM value in gamma band among PD-CI, PD-NC, and HS. The upper and lower bound of the box refer to the 25th to 75th percentiles, the median value is represented by the horizontal line inside each box, the whiskers extend to the 10th and 90th percentiles, and further data are considered as outliers and represented by the symbol +. The PD-CI group shows lower nodal PLM values in fusiform gyrus, Heschl's gyrus, inferior temporal gyrus, post-central gyrus, and lingual gyrus, on the left, as compared with both PD-NC group and HS. $*p<0.05$, $**p<0.01$, $***p<0.001$. Color images are available online.
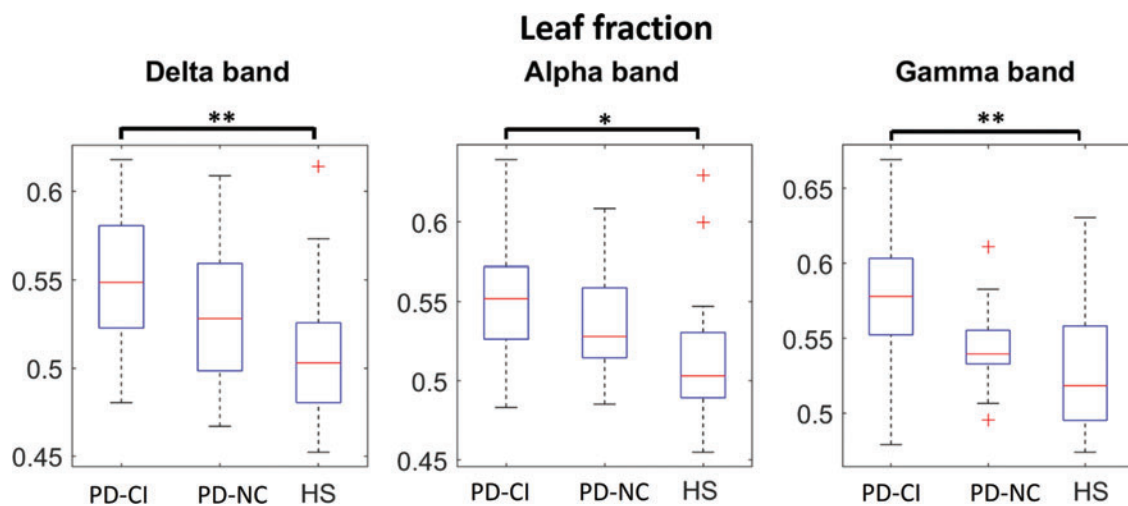

FIG. 3. Differences in leaf fraction parameter, among PD-CI, PD-NC, and HS. The box plots refer to differences in the Lf among, respectively, PD-CI, PD-NC, and HS. The upper and lower bound of the box refer to the 25th to 75th percentiles, the median value is represented by the horizontal line inside each box, the whiskers extend to the 10th and 90th percentiles, and further data are considered as outliers and represented by the symbol +. The PD-CI group shows a higher Lf, compared with both PD-NC group and HS, in delta, alpha, and gamma band. $*p<0.05$, $**p<0.01$. Color images are available online.

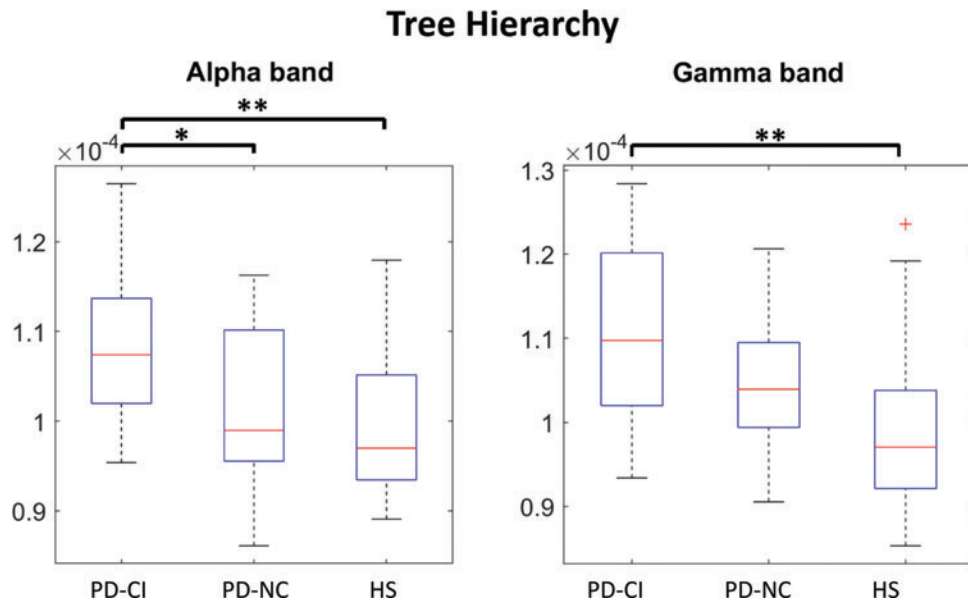**6**

Tree Hierarchy

FIG. 4. Differences in Th parameter among PD-CI, PD-NC, and HS. The box plots refer to differences in the Th among, respectively, PD-CI, PD-NC, and HS. The upper and lower bound of the box refer to the 25th to 75th percentiles, the median value is represented by the horizontal line inside each box, the whiskers extend to the 10th and 90th percentiles, and further data are considered as outliers and represented by the symbol +. The PD-CI group shows a higher Th, compared with both PD-NC group and HS, in the alpha and gamma bands. $*p < 0.05$, $**p < 0.01$. Th, tree hierarchy. Color images are available online.
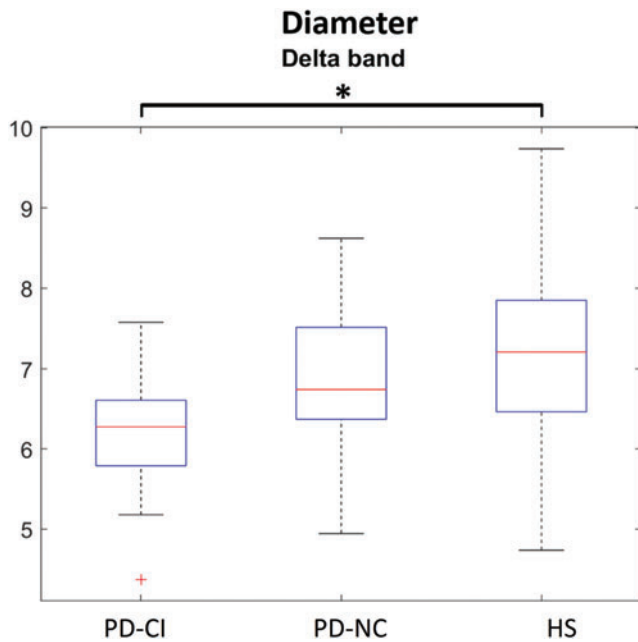

FIG. 5. Differences in diameter in PD-CI, PD-NC, and HS. The box plots refer to differences in the D among, respectively, PD-CI, PD-NC, and HS. The upper and lower bound of the box refer to the 25th to 75th percentiles, the median value is represented by the horizontal line inside each box, the whiskers extend to the 10th and 90th percentiles, and further data are considered as outliers and represented by the symbol +. The PD-CI group shows a statistically significant lower diameter compared with both PD-NC group and HS, in delta band. $*p < 0.05$. Color images are available online.

In addition, as reported in Table 2, when we performed a multivariate regression analysis, we found that only the Th in the alpha band can predict the MoCA scores, with a p-value = 0.005, $R^2 = 0.214$, and $B = -21.873$.

Discussion

Our study was designed to test the hypothesis that the cognitive decline observed in PD patients may be associated to specific changes of both functional connectivity and brain topology. Further, we hypothesized that the extent of brain network alterations may be correlated with the cognitive outcome. By applying the PLM, a connectivity metric that measures the synchronization between brain regions (Baselice et al., 2019) to MEG signals, we were able to highlight differences in the global and nodal PLM values in PD-CI as compared with both PD-NC and HS. Further, using graph analysis, we found specific PD-related changes in brain network topology that were related to cognitive functioning.

Functional connectivity. We found that the global PLM value in the gamma band was significantly reduced in PD-CI patients as compared with HS. This measure, obtained by averaging over all 90 (one for each ROI) nodal PLM values, is a measure of global functional connectivity. Interestingly, the global PLM of PD-NC patients was intermediate between that of HS and PD-CI (although the difference was not statistically significant).

The nodal PLM values showed a similar trend to that of the global PLM. For example, the nodal PLM of cognitively PD-NC patients was intermediate between PD-CI patients

FIG. 6. Spearman's rank correlation coefficient. The MoCA test correlates positively with the diameter ($R = 0.352$, $p = 0.028$) and negatively with the Th ($R = 0.374$, $p = 0.019$). Color images are available online.
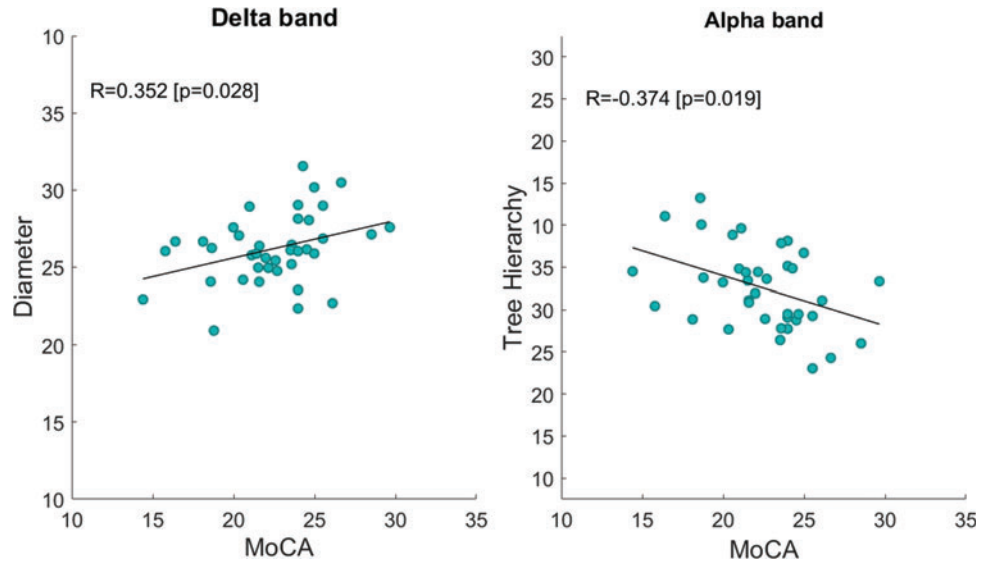
and HS in the gamma band. Specifically, a statically significant reduction of the functional connectivity was observed in several temporal (fusiform gyrus, Heschl's gyrus, and inferior temporal gyrus), parietal (postcentral gyrus), and occipital (lingual gyrus) areas within the left hemisphere, as compared with HS. Moreover, the PLM of the lingual and fusiform left gyri was significantly reduced with respect to the HS in both PD-CI and PD-NC patients (Fig. 2).

The heterogeneity of the clinical onset, the prognostic evolution, as well as the response to dopaminergic therapy suggest the existence of two distinct cognitive syndromes in PD (although with overlapping elements), namely the frontostriatal syndrome (Tessitore et al., 2012b) and the posterior cortical syndrome (Baggio et al., 2015; Tremblay et al., 2013). The former is cognitively characterized mainly by dysexecutive disorders, and it is strictly related to the dopaminergic imbalance (Gotham et al., 1986); however, in the latter, memory deficit, visuospatial/visuoperceptual disturbances, and, more generally, global cognitive decline are frequently observed (Williams-Gray et al., 2009).

Importantly, the posterior cortical syndrome is associated with a worse cognitive prognosis (Kehagia et al., 2010).

Overall, our results are in line with this view, where the form presenting the greater risk of developing dementia (Olde Dubbelink et al., 2014) showed widespread functional connectivity in temporal, parietal, and occipital regions (Baggio et al., 2015). Interestingly, cortical areas showing reduced synchronization in cognitively impaired PD subjects (i.e., fusiform gyrus, Heschl's gyrus, inferior temporal gyrus, postcentral gyrus, and lingual gyrus) are mainly involved in the posterior cortical syndrome.

Taking into account the clinical evidence suggesting that damage in such regions leads to severe cognitive impairment with a high risk of developing dementia, we might speculate that, if these regions are less integrated with the rest of the brain, then the cognitive functioning might be impaired. This is also supported by our correlation analysis, showing that the less the synchronization between these areas and the rest of the brain, the worst the cognitive performance.

It is important to note that there was a clear downward trend between HS and all PD in both global and nodal PLM values, with the PD-NC group always displaying intermediate values. This observation could suggest that the reduction of the functional connectivity in terms of reduced

TABLE 2. RESULTS OF THE MULTIVARIATE REGRESSION ANALYSIS

Frequency band	Parameter	B	R^2	p
Delta	Diameter	1.189	0.129	0.058
	Leaf fraction	−5.883		0.668
Alpha	Leaf fraction	28.516	0.214	0.144
	Tree hierarchy	−21.873		**0.005**
Gamma	Leaf fraction	2.170	0.023	0.920
	Tree hierarchy	−5.906		0.538
	Global PLM	−418.757	0.195	0.063
	Nodal PLM of left post-central gyrus	138.701		0.168
	Nodal PLM of left lingual gyrus	18.806		0.879
	Nodal PLM of left fusiform gyrus	−53.060		0.722
	Nodal PLM of left Heschl's gyrus	152.485		0.258
	Nodal PLM of left inferior temporal gyrus	210.021		0.159

The bold indicates $p < 0.05$.
PLM, phase linearity measurement.

overall synchronization (estimated by the PLM) progresses till it exceeds a threshold, and the cognitive impairment acquires clinical significance (Sorrentino et al., 2021).

It is even more interesting to observe that the reduction in synchronization in the posterior regions (along with the cognitive impairment) is not a function of disease progression or severity, as documented by the comparison of the clinical scales between the two PD groups. Finally, it is worth noting that all these results are in the gamma band (30–48 Hz), which has been related to visual perception, attention, auditory processing, learning, and memory (Hoogenboom et al., 2006; Kaiser and Lutzenberger, 2005).

Brain network topology. The reduction of functional connectivity in PD patients is linked to changes in the large-scale functional organization of the brain, as captured by our topological network results. With regard to the centrality parameters (degree and BC), which evaluate the topological characteristic of each single region, we did not find any statistically significant difference among the three groups. However, with regard to the global parameters, expressing global topological features of the brain network, PD-CI patients, as compared with HS and PD-NC patients, showed widespread differences in multi-frequencies bands (delta, alpha, gamma) in the Lf, Th (both higher in PD-CI), and diameter (lower in PD-CI) (Figs. 3–5).

It should be noted that, similarly to the functional connectivity, the PD-NC group shows an intermediate profile between HS and PD-CI, even when the difference does not reach statistical significance (Fig. 4).

The Lf is defined as the ratio between the number of leaf nodes (nodes with degree = 1) and the maximum possible number of links (total number of nodes minus 1). An Lf equal to 1 indicates a network with a star-like topology (Tewarie et al., 2015), where each couple of nodes is topologically closer, and the shortest path passes on a small subset of highly important nodes. On the contrary, an Lf equal to 0 signifies a line-like network, which is less reliant on any singly node, and hence with higher resiliency to targeted attacks (Rubinov and Sporns, 2010; Tononi et al., 1994).

Related to the Lf, the diameter provides information about the distance between all pairs of nodes. In fact, lower diameter, as shown by PD patients in the delta band, is indicating a more compact, star-like network (Boersma et al., 2013).

Finally, the Th quantifies the trade-off between efficient communication (large-scale integration) and prevention of the overload of the most important nodes. A higher Th, as found in PD-CI, may suggest a sub-optimal balance, with respect to both PD-NC (in the alpha band) and HS (in the alpha and the gamma band), in the sense that, in pathology, the network integration becomes reliant on a small subset of important areas, hence losing resiliency. This mechanism might underlie the reduction of functional connectivity found in some brain areas (Figs. 1 and 2) linked to cognitive deterioration.

Correlation and multivariate regression analysis. Interestingly, as reported in Figure 6, we found a statistically significant correlation between the MoCA test and both the diameter in the delta band (direct correlation) and the Th in the alpha band (inverse correlation). These correlations are in line with our findings and support the hypothesis of reduced synchronization in some brain areas, as well as

hyperconnected network topology, which might capture sub-optimal large-scale functional organization underpinning cognitive impairment development in PD patients. This hypothesis is corroborated also by the results of the multivariate regression analysis, which reinforces the idea that in PD-CI the cognitive impairment is somewhat related to a reconfiguration of the brain network.

Conclusion

In conclusion, in this work, we show that in PD patients in the early phase of the disease, the functional connectivity changes, as well as the topological rearrangements within the large-scale functional networks, are correlated to cognitive impairment. In particular, we found reduced functional connectivity in PD-CI (with respect to both PD-NC and HS) in terms of reduced overall synchronization, as estimated by the PLM, as well as specifically in the posterior hubs. Further, analyzing the brain networks, we found a more star-like topology in PD-CI.

It is noteworthy to observe that both PD groups (i.e., PD-CI and the PD-NC group) did not differ with regard to the disease stage as well as to the motor impairment. Nonetheless, the group affected by earlier development of cognitive impairment was the one showing reduced synchronization in the posterior areas. These data are in line with the hypothesis that two distinct clinical phenotypes (although with overlapping elements) exist and that involvement of the posterior regions relates to earlier cognitive decline.

Limitations and future directions

Our article shows the relevance of topological analysis of the brain functional networks to find correlates of the cognitive impairment in PD. However, some limitations should be highlighted. First, it is important to note that our study relies on source-reconstructed data. Hence, caution should be used when interpreting the results of deep sources, which will have a lower signal-to-noise ratio as compared with cortical sources.

Further, in this study we used the AAL, which a relative course-grained atlas. Although this is imposed by the spatial resolution of the MEG, further studies using modalities with higher spatial resolution should complement our findings.

Finally, applying the use of topological analysis to find neurophysiological correlates of cognitive impairment in neurodegeneration is a promising venue for future investigation. In fact, it should be investigated whether the alterations we report in the large-scale brain organization are disease-specific or they point to more general mechanisms. To this end, different kinds of neurological diseases as well as specific kinds of cognitive impairment could be investigated by using this approach in the future.

Data Availability

The MEG data and the reconstructed avalanches are available on reasonable request to the corresponding author, conditional on appropriate ethics approval at the local site.

Disclaimer

The material presented has not been published or submitted for publication elsewhere, except on the pre-print server BiorXiv at the following link: https://doi.org/10.1101/2020.12.14.422706.

Author Disclosure Statement

No competing financial interests exist.

Funding Information

This study was funded by the University of Naples Parthenope within the Project "Bando Ricerca Competitiva 2017" (D.R. 289/2017).

References

Aarsland D, Brønnick K, Larsen JP, et al. 2009. Cognitive impairment in incident, untreated Parkinson disease: the Norwegian ParkWest study. Neurology 72:1121–1126.

Aarsland D, Kurz MW. 2010. The epidemiology of dementia associated with Parkinson disease. J Neurol Sci 289:18–22.

Amboni M, Iuppariello L, Iavarone A, et al. 2018. Step length predicts executive dysfunction in Parkinson's disease: a 3-year prospective study. J Neurol 265:2211–2220.

Amico E, Goñi J. 2018. The quest for identifiability in human functional connectomes. Sci Rep 8:1–14.

Azarpaikan A, Torbati HT, Sohrabi M. 2014. Neurofeedback and physical balance in Parkinson's patients. Gait Posture 40:177–181.

Baggio HC, Segura B, Garrido-Millan JL, et al. 2015. Resting-state frontostriatal functional connectivity in Parkinson's disease-related apathy. Mov Disord 30:671–679.

Baillet S. 2017. Magnetoencephalography for brain electrophysiology and imaging. Nat Neurosci 20:327–339.

Barbati G, Porcaro C, Zappasodi F, et al. 2004. Optimization of an independent component analysis approach for artifact identification and removal in magnetoencephalographic signals. Clin Neurophysiol 115:1220–1232.

Baselice F, Sorriso A, Rucco R, et al. 2019. Phase linearity measurement: a novel index for brain functional connectivity. IEEE Trans Med Imaging 38:873–882.

Beck AT, Ward CH, Mendelson M, et al. 1961. An inventory for measuring depression. Arch Gen Psychiatry 4:561–571.

Benjamini Y, Hochberg Y. 1995. Controlling the false discovery rate: a practical and powerful approach to multiple testing. Source J Royal Stat Soc Ser B 57:289–300.

Boersma M, Smit DJA, Boomsma DI, et al. 2013. Growing trees in child brains: graph theoretical analysis of electroencephalography-derived minimum spanning tree in 5- and 7-year-old children reflects brain maturation. Brain Connect 3:50–60.

Bosboom JLW, Stoffers D, Stam CJ, et al. 2006. Resting state oscillatory brain dynamics in Parkinson's disease: an MEG study. Clin Neurophysiol 117:2521–2531.

Braak H, Del Tredici K, Rüb U, et al. 2003. Staging of brain pathology related to sporadic Parkinson's disease. Neurobiol Aging 24:197–211.

Buzsáki G, Draguhn A. 2004. Neuronal olscillations in cortical networks. Science (80−) 304:1926–1929.

Conti S, Bonazzi S, Laiacona M, et al. 2015. Montreal Cognitive Assessment (MoCA)-Italian version: regression based norms and equivalent scores. Neurol Sci 36:209–214.

de Cheveigné A, Simon JZ. 2007. Denoising based on time-shift PCA. J Neurosci Methods 165:297–305.

Dubbelink KTEO, Stoffers D, Deijen JB, et al. 2013. Cognitive decline in Parkinson's disease is associated with slowing of resting-state brain activity: a longitudinal study. Neurobiol Aging 34:408–418.

Emre M, Aarsland D, Brown R, et al. 2007. Clinical diagnostic criteria for dementia associated with Parkinson's disease. Mov Disord 22:1689–1707.

Fahn SRLE. 1987. Members of the UPDRS development committee. Unified Parkinson's disease rating scale. Recent developments in Parkinson's disease 2:293–304.

Fallani FDV, Latora V, Chavez M. 2017. A topological criterion for filtering information in complex brain networks. PLoS Comput Biol 13:e1005305.

Freeman LC. 1977. A set of measures of centrality based on betweenness. Sociometry 40:35.

Gibb WR, Lees AJ. 1988. A comparison of clinical and pathological features of young- and old-onset Parkinson's disease. Neurology 38:1402–1406.

Gong G, He Y, Concha L, et al. 2009. Mapping anatomical connectivity patterns of human cerebral cortex using in vivo diffusion tensor imaging tractography. Cereb Cortex 19:524–536.

Gotham A-M, Brown RG, Marsden CD. 1986. Levodopa treatment may benefit or impair'' frontal'' function in Parkinson's disease. Lancet 328:970–971.

Gross J, Baillet S, Barnes GR, et al. 2013. Good practice for conducting and reporting MEG research. Neuroimage 65:349–363.

Hoehn MM, Yahr MD. 1967. Parkinsonism: onset, progression, and mortality. Neurology 17:427.

Hoogenboom N, Schoffelen J-M, Oostenveld R, et al. 2006. Localizing human visual gamma-band activity in frequency, time and space. Neuroimage 29:764–773.

Jacini F, Sorrentino P, Lardone A, et al. 2018. Amnestic mild cognitive impairment is associated with frequency-specific brain network alterations in temporal poles. Front Aging Neurosci 10:400.

Kaiser J, Lutzenberger W. 2005. Human gamma-band activity: a window to cognitive processing. Neuroreport 16:207–211.

Kehagia AA, Barker RA, Robbins TW. 2010. Neuropsychological and clinical heterogeneity of cognitive impairment and dementia in patients with Parkinson's disease. Lancet Neurol 9:1200–1213.

Lardone A, Liparoti M, Sorrentino P, et al. 2018. Mindfulness meditation is related to long-lasting changes in hippocampal functional topology during resting state: a magnetoencephalography study. Neural Plast 2018:5340717.

Lopes da Silva F. 2013. EEG and MEG: relevance to neuroscience. Neuron 80:1112–1128.

Marin RS, Biedrzycki RC, Firinciogullari S. 1991. Reliability and validity of the Apathy Evaluation Scale. Psychiatry Res 38:143–162.

Nasreddine ZS, Phillips NA, Bédirian V, et al. 2005. The Montreal Cognitive Assessment, MoCA: a Brief Screening Tool for mild cognitive impairment. J Am Geriatr Soc 53:695–699.

Nolte G. 2003. The magnetic lead field theorem in the quasi-static approximation and its use for magnetoencephalography

forward calculation in realistic volume conductors. Phys Med Biol 48:3637–3652.

Olde Dubbelink KTE, Hillebrand A, Stoffers D, et al. 2014. Disrupted brain network topology in Parkinson's disease: a longitudinal magnetoencephalography study. Brain 137:197–207.

Oostenveld R, Fries P, Maris E, et al. 2011. FieldTrip: open source software for advanced analysis of MEG, EEG, and invasive electrophysiological data. Comput Intell Neurosci 2011:156869.

Pievani M, Filippini N, Van Den Heuvel MP, et al. 2014. Brain connectivity in neurodegenerative diseases—from phenotype to proteinopathy. Nat Rev Neurol 10:620–633.

Roth M, Tym E, Mountjoy CQ, et al. 1986. CAMDEX: a standardised instrument for the diagnosis of mental disorder in the elderly with special reference to the early detection of dementia. Br J Psychiatry 149:698–709.

Rubinov M, Sporns O. 2010. Complex network measures of brain connectivity: uses and interpretations. Neuroimage 52:1059–1069.

Rucco R, Liparoti M, Jacini F, et al. 2019. Mutations in the SPAST gene causing hereditary spastic paraplegia are related to global topological alterations in brain functional networks. Neurol Sci 40:979–984.

Sadasivan PK, Dutt DN. 1996. SVD based technique for noise reduction in electroencephalographic signals. Signal Process 55:179–189.

Shen X, Finn ES, Scheinost D, et al. 2017. Using connectome-based predictive modeling to predict individual behavior from brain connectivity. Nat Protoc 12:506–518.

Singer W. 1999. Neuronal synchrony: a versatile code for the definition of relations? Neuron 24:49–65.

Sorrentino P, Nieboer D, Twisk JWR, et al. 2017. The hierarchy of brain networks is related to insulin growth factor-1 in a large, middle-aged, healthy cohort: an Exploratory Magneto-encephalography Study. Brain Connect 7:321–330.

Sorrentino P, Rucco R, Baselice F, et al. 2021. Flexible brain dynamics underpins complex behaviours as observed in Parkinson's disease. Sci Rep 11:1–12.

Sorrentino P, Rucco R, Jacini F, et al. 2018. Brain functional networks become more connected as amyotrophic lateral sclerosis progresses: a source level magnetoencephalographic study. Neuroimage Clin 20:564–571.

Sporns O, Tononi G, Kötter R. 2005. The human connectome: a structural description of the human brain. PLoS Comput Biol 1:e42.

Stam CJ, Tewarie P, Van Dellen E, et al. 2014. The trees and the forest: characterization of complex brain networks with minimum spanning trees. Int J Psychophysiol 92:129–138.

Stoffers D, Bosboom JLW, Deijen JB, et al. 2007. Slowing of oscillatory brain activity is a stable characteristic of Parkinson's disease without dementia. Brain 130:1847–1860.

Tessitore A, Amboni M, Esposito F, et al. 2012a. Resting-state brain connectivity in patients with Parkinson's disease and freezing of gait. Parkinsonism Relat Disord 18:781–787.

Tessitore A, Esposito F, Vitale C, et al. 2012b. Default-mode network connectivity in cognitively unimpaired patients with Parkinson disease. Neurology 79:2226–2232.

Tewarie P, van Dellen E, Hillebrand A, et al. 2015. The minimum spanning tree: an unbiased method for brain network analysis. Neuroimage 104:177–188.

Tomlinson CL, Stowe R, Patel S, et al. 2010. Systematic review of levodopa dose equivalency reporting in Parkinson's disease. Mov Disord 25:2649–2653.

Tononi G, Sporns O, Edelman GM. 1994. A measure for brain complexity: relating functional segregation and integration in the nervous system. Proc Natl Acad Sci 91:5033–5037.

Tremblay C, Achim AM, Macoir J, et al. 2013. The heterogeneity of cognitive symptoms in Parkinson's disease: a meta-analysis. J Neurol Neurosurg Psychiatry 84:1265–1272.

Tzourio-Mazoyer N, Landeau B, Papathanassiou, D., et al. 2002. Automated anatomical labeling of activations in SPM using a macroscopic anatomical parcellation of the MNI MRI single-subject brain. Neuroimage 15:273–289.

Van Veen BD, Van Drongelen W, Yuchtman M, et al. 1997. Localization of brain electrical activity via linearly constrained minimum variance spatial filtering. IEEE Trans Biomed Eng 44:867–880.

Varela F, Lachaux J-P, Rodriguez E, et al. 2001. The brainweb: phase synchronization and large-scale integration. Nat Rev Neurosci 2:229.

Vitale C, Agosti V, Avella D, et al. 2012. Effect of Global Postural Rehabilitation program on spatiotemporal gait parameters of parkinsonian patients: a three-dimensional motion analysis study. Neurol Sci 33:1337–1343.

Walshe FMR. 1961. Contributions of John Hughlings Jackson to neurology: a brief introduction to his teachings. Arch Neurol 5:119–131.

Williams-Gray CH, Evans JR, Goris A, et al. 2009. The distinct cognitive syndromes of Parkinson's disease: 5 year follow-up of the CamPaIGN cohort. Brain 132:2958–2969.

Address correspondence to:
Giuseppe Sorrentino
Department of Motor Sciences and Wellness
University of Naples Parthenope
Via Medina 40, 80133 Naples
Italy

E-mail: giuseppe.sorrentino@uniparthenope.it